Beyond SCR in Weak Grids: Analytical Evaluation of Voltage Stability and Excess System Strength

Boricic, Aleksandar; Rueda Torres, José Luis; Popov, Marjan

DOI
10.1109/FES57669.2023.10183286

Publication date
2023

Document Version
Final published version

Published in
Proceedings of the 2023 International Conference on Future Energy Solutions (FES)

Beyond SCR in Weak Grids: Analytical Evaluation of Voltage Stability and Excess System Strength

Aleksandar Boričić
Faculty of EEMCS
Delft University of Technology
Delft, The Netherlands
A.Boricic@tudelft.nl

Jose Luis Rueda Torres
Faculty of EEMCS
Delft University of Technology
Delft, The Netherlands
J.L.RuedaTorres@tudelft.nl

Marjan Popov
Faculty of EEMCS
Delft University of Technology
Delft, The Netherlands
M.Popov@tudelft.nl

2023 International Conference on Future Energy Solutions (FES) | 979-8-3503-3230-8/23/$31.00 ©2023 IEEE | DOI: 10.1109/FES57669.2023.10183286

***Abstract*— Due to the continuous increase (decrease) in the number of inverter-based (synchronous) generators in modern electrical power systems, the theoretical foundations behind widely used system strength and voltage stability assessment methods require thorough revision. The existing evaluation methods such as the Short-Circuit Ratio (SCR) are often based on simplifications which may produce inaccuracies, particularly when studying weak systems. As a result, a misleading estimation of voltage stability can occur, exposing systems to unnecessary renewables curtailment or other inappropriate remedial actions that may cause partial disruptions or potential instability. This paper provides a rigorous analytical revision of voltage stability assessment to confidently evaluate the maximum power transfer under various operating conditions. Subsequently, the proposed approach is applied as an enhanced method of system strength evaluation. The method is extensively tested on a single-machine-infinite-bus test system. Numerical results show a notably more accurate assessment relative to the common alternative methods.**

***Index Terms*—System Strength, Voltage Stability, Weak Grids, Voltage Collapse, Inverter-based Resources**

I. Introduction

Decarbonization of the electricity supply exposes power systems to unprecedented changes. The number of Inverter-Based Resources (IBRs) increases rapidly as a replacement for a fossil-based synchronous generation. An often-encountered challenge in such modern power systems is voltage stability [1-4]. The measure of voltage stability resilience is often described as *system strength*, analogous to inertia and frequency stability [5-9]. System strength is, however, a complex concept with distinct steady- and dynamic-state characteristics [9]. This paper focuses on steady-state characteristics. The dynamic performance is discussed in [8-11]. Other aspects of low system strength, such as protection misoperation [12, 13] and power quality deterioration [6], fall beyond the scope of this paper.

A common metric to evaluate system strength is Short-Circuit Ratio (SCR) [5]. However, SCR is merely a convenient simplification of system strength. Recent research highlights some of its main drawbacks, particularly for the analysis of weaker grids [9, 14-15]. New methods to tackle these challenges emerge, such as voltage sensitivity [15], generalized SCR [16], and many more, with an overview in [9, 14]. As SCR is unable to take into account shunt capacitors, methods like Effective SCR (ESCR) were proposed [17]. Moreover, the grid X/R ratio is often neglected. The impact of multiple IBRs on system strength is explored extensively in [18]. Finally, load plays an important role in system strength evaluation, however, its impact is often not captured by existing methods [15, 19]. Therefore, most of the existing methods fail to capture the full scope of steady state system strength. This may result in a misestimation of both system strength and voltage stability.

The result is an increased risk of voltage instabilities [1-3]. Alternatively, as the curtailment of renewables becomes more common to preserve sufficient SCR [10, 14], renewable sources may end up underexploited due to potentially misleading outcomes obtained by system strength evaluation methods.

In this paper, an extensive and rigorous analytical derivation of maximum power transfer considering voltage stability limits is presented. This approach is further utilized to derive a novel and more accurate system strength evaluation method.

The paper is divided into four sections. Section II provides a detailed analytical derivation of voltage stability boundaries. In Section III, the impacts of loads, capacitors, and the X/R ratio are explored. In Section IV, a novel system strength method is introduced and extensively validated. Finally, conclusions and future research directions are presented in the last section.

II. Steady-state voltage stability limitations

For derivation and demonstration of the applied analysis, a single-IBR-infinite-bus system is used, as shown in Fig. 1. Based on this system, the following equations are written:

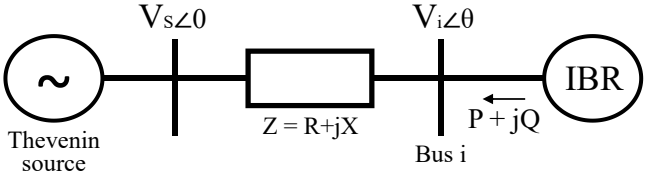

Figure 1. IBR grid connection, represented by a Thevenin equivalent.

$$\frac{\underline{V_i}-\underline{V_s}}{\underline{Z}}=\underline{I}=\left(\frac{\underline{S}}{\underline{V_i}}\right)^*\rightarrow\underline{S}=\underline{V_i}\frac{\underline{V_i}^*-\underline{V_s}^*}{\underline{Z}^*}=P+jQ \quad (1)$$

This work was financially supported by the Dutch Scientific Council NWO in collaboration with TSO TenneT, DSOs Alliander, Stedin, Enduris, VSL and General Electric in the framework of the Energy System Integration & Big Data program under the project "Resilient Synchromeasurement-based Grid Protection Platform, no. 647.003.004".

$$\underline{S} = (V_i cos\theta + jV_i sin\theta)\frac{V_i cos\theta - jV_i sin\theta - V_s}{R - jX} \quad (2)$$

$$\alpha = {}^{R}/_{Z^2} \quad ; \quad \beta = {}^{X}/_{Z^2} \quad (3)$$

By separating real and imaginary parts of (2) and combining those with (3), (4) and (5) are derived for active/reactive power.

$$P = \alpha(V_i^2 - V_i V_s cos\theta) + \beta V_i V_s sin\theta \quad (4)$$

$$Q = \beta(V_i^2 - V_i V_s cos\theta) - \alpha V_i V_s sin\theta \quad (5)$$

If $R \approx 0$ is assumed, this simplifies to the expressions in (6). The impact of $R > 0$ is investigated in Section III.

$$P = \frac{V_i V_s sin\theta}{X} \quad ; \quad Q = \frac{V_i^2 - V_i V_s cos\theta}{X} \quad (6)$$

Expression (6) dictates the maximum active power transfer with respect to the angle stability, and the necessary reactive power to sustain that transfer. However, these expressions do *not* consider static voltage stability. To derive voltage stability limits, inspired by the approach in [18], (1) can be rewritten as:

$$\underline{Z}\,\underline{S}^* = V_i^2 - \underline{V_s}\,\underline{V_i}^* \quad (7)$$

If $\underline{Z}\,\underline{S}^* = a - jb$, where a and b are real numbers, real and imaginary parts of (7) can be separated as in (8) and (9).

$$a = V_i^2 - V_s V_i cos\theta = f_1(V_i, \theta) \quad (8)$$

$$b = V_s V_i sin\theta = f_2(V_i, \theta) \quad (9)$$

The Jacobian matrix of $\boldsymbol{f} = [f_1, f_2]^T$ is further derived:

$$\boldsymbol{J} = \begin{bmatrix} \frac{\partial f_1}{\partial V_i} & \frac{\partial f_1}{\partial \theta} \\ \frac{\partial f_2}{\partial V_i} & \frac{\partial f_2}{\partial \theta} \end{bmatrix} = \begin{bmatrix} 2V_i - V_s cos\theta & V_s V_i sin\theta \\ V_s sin\theta & V_s V_i cos\theta \end{bmatrix} \quad (10)$$

A singular Jacobian matrix indicates a system voltage instability condition. The stability boundary is therefore found by solving the $\det(\boldsymbol{J}) = 0$ expression, and is shown in (11).

$$cos\theta = \frac{1}{2}\frac{V_s}{V_i} \rightarrow \theta_{max} = acos(\frac{1}{2}\frac{V_s}{V_i}) \quad (11)$$

For a base case $V_i = V_s = 1\,pu$, the maximum angle equals 60°. This is *lower* than the angle stability limitation of 90° implied by the active power computed by (6). We, therefore, extend this approach further by incorporating the voltage stability boundary (11) into the power transfer (6) equation:

$$P_{max} = \frac{V_i V_s sin\theta_{max}}{X} = \frac{V_i V_s \sin(acos\left(\frac{1}{2}\frac{V_s}{V_i}\right))}{X} \quad (12)$$

By using the trigonometric identity $\sin(acos(x)) = \sqrt{1 - x^2}$, a novel expression for static voltage stability limit in terms of maximum power transfer is derived in (13).

$$P_{max} = \frac{1}{X} V_i V_s \sqrt{1 - \left(\frac{1}{2}\frac{V_s}{V_i}\right)^2} \quad (13)$$

For transferring $P = P_{max}$ in (13), the reactive power required to maintain the voltage can be computed by combining (6) and (11), as shown in (14):

$$Q_{P=P_{max}} = \frac{V_i^2 - V_i V_s cos\theta_{max}}{X} = \frac{1}{X}(V_i^2 - \frac{V_s^2}{2}) \quad (14)$$

For an illustrative case with parameters $S_{sc} = V_i = V_s = X = 1\,pu$, P_{max} is computed for the boundary stability condition based on the SCR metric and compared to (13):

$$SCR = 1 = \frac{S_{sc}}{P_{max}} = \frac{{V_{i_{nom}}^2}/{X}}{P_{max}} \rightarrow P_{max} = 1\,pu \quad (15)$$

$$P_{max} = \frac{1}{X} V_i V_s \sqrt{1 - \left(\frac{1}{2}\frac{V_s}{V_i}\right)^2} = \frac{\sqrt{3}}{2} = 0.866\,pu \quad (16)$$

The maximum power transfer is *lower* than what the SCR implies. This is due to an IBR being a PQ source, rather than a PV source. In other words, IBR does not behave as a voltage source but is instead perceived as a current source from the bulk power system perspective. This fundamentally differs from a synchronous generator electromagnetically coupled to the grid, which would be able to operate at $P_{max} \approx 1\,pu$ in a similar case.

SCR is therefore an over-optimistic measure of system strength and the voltage collapse boundary with IBRs. Furthermore, SCR does not take into consideration the actual operating voltage V_i. Meanwhile, expression (13) does. The relation is depicted in Fig. 2, by plotting the function $P_{max} = f(V_i)$ for a per-unit system with base $S_{sc} = X = V_s = 1$.

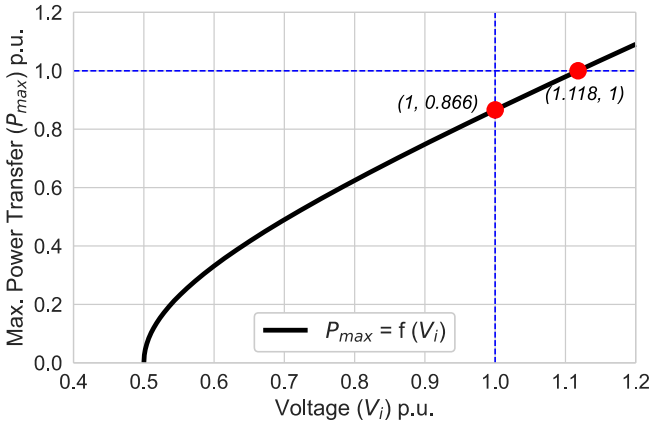

Figure 2. Maximum power transfer as a function of operating voltage.

For $V_i = 1\,pu$, a maximum of $P = 0.866\,pu$ can be transferred, as shown in (16). Furthermore, transferring $P = S_{sc} = 1\,pu$ (as implied by SCR) would result in a voltage collapse for $V_i = 1\,pu$. Instead, the voltage would need to be higher ($V_i = 1.118\,pu$) for such a transfer to be feasible from a voltage stability perspective. Therefore, in a lossless system with a PQ source supplying power to the grid, the SCR method is an over-optimistic measure of system strength. In contrast, the derived approach (13) shows high accuracy. The analytical expressions are validated through simulations in Section IV.

III. Impact of Loads, Capacitors and the X/R Ratio

Section II explores the maximum power transfer by assuming there are no shunt elements like loads or capacitors,

and that the system impedance is dominantly reactive ($R \approx 0$). In this section, it is further explored how these assumptions affect the maximum power transfer and system strength.

A. Impact of local loads on system strength

The system shown in Fig. 1 is altered with the addition of a local load at bus i ($P_L > 0$). Deriving the boundary condition for such a case is relatively simple. What matters for the voltage stability is the power transfer towards the system, from the system perspective. In other words, the *net* maximum active power transfer. This can be calculated as proposed in (17):

$$P_{net\_max} = P_{max} + P_L \tag{17}$$

The maximum power transfer with a load included is evaluated analytically for a load of $P_L = 0.2\,pu$. The results are shown in Fig. 3. For nominal voltage, voltage collapse occurs at power transfer $P_{net\_max} = 1.066$ (dashed line), which is precisely in line with (16) and (17). Furthermore, it can be seen that the entire plot from Fig. 2 is shifted upwards by the value of P_L, in line with the analytical expressions (16) and (17).

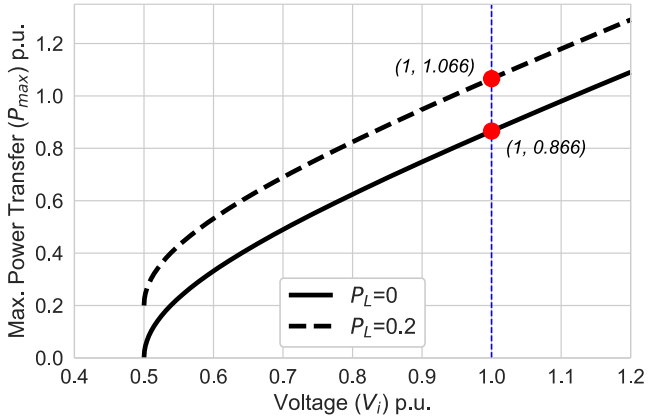

Figure 3. Maximum power transfer as a function of operating voltage V_i with the presence of a local load.

It is important to note that a constant active power load is assumed. If there is a voltage dependence, it should be reflected as $P_L = f(V_i)$ relation. Nevertheless, the derived relationship (17) holds for such a case as well. However, the upward shift in Fig. 3 would not be distributed equally along the curve.

B. Impact of capacitors on system strength

The impact of shunt capacitance is evaluated now, assuming a capacitor $Q_c > 0$ connected in parallel at bus i in Fig. 1. Q_c can be expressed as $Q_c = {V_i^2}/{X_C}$, where X_C is the capacitive reactance. To derive the boundary voltage stability condition, the impedance equivalent is first derived, as shown in (18).

$$\underline{Z'} = \underline{Z_L} || \underline{Z_c} = \frac{jX_L * (-jX_c)}{jX_L + (-jX_c)} = j\frac{X_L X_c}{X_C - X_L} \tag{18}$$

Alternatively, with the nominal reactive power of the capacitor $Q_{C_{nom}} = {V_{i_{nom}}^2}/{X_C}$, (18) can be rewritten as (19):

$$Z' = \frac{X_L X_c}{X_C - X_L} = \frac{X_L}{1 - X_L/X_C} = \frac{X_L}{1 - \frac{X_L Q_{C_{nom}}}{V_{i_{nom}}^2}} \tag{19}$$

Using the voltage divider principle, the new Thevenin source voltage is derived in (20) and (21).

$$V_s' = V_s \frac{Z'}{Z} = V_s \frac{1}{1 - \frac{X_L Q_{C_{nom}}}{V_{i_{nom}}^2}} = \frac{V_s}{1 - f_C} \tag{20}$$

$$f_C = X_L/X_C = \frac{X_L Q_{C_{nom}}}{V_{i_{nom}}^2} \tag{21}$$

By inserting (19) and (20) into (13), (22) is obtained, which is the novel analytical expression of the maximum active power transfer in the presence of a shunt capacitor.

$$P_{max} = \frac{1}{X} V_i V_s \sqrt{1 - \left(\frac{1}{2}\frac{V_s}{V_i(1 - f_C)}\right)^2} \tag{22}$$

The necessary reactive power to sustain this active power flow is calculated by inserting (19) and (20) into the expression (14).

$$Q_{P=P_{max}} = \frac{1 - f_C}{X}\left[V_i^2 - \frac{1}{2}\left(\frac{V_s}{1 - f_C}\right)^2\right] \tag{23}$$

This dependence is visualized in Fig. 4 ($S_{sc} = V_i = V_s = 1\,pu$). The Y-axis depicts the maximum power transfer for the reactive power compensation in per-unit values shown on the X-axis.

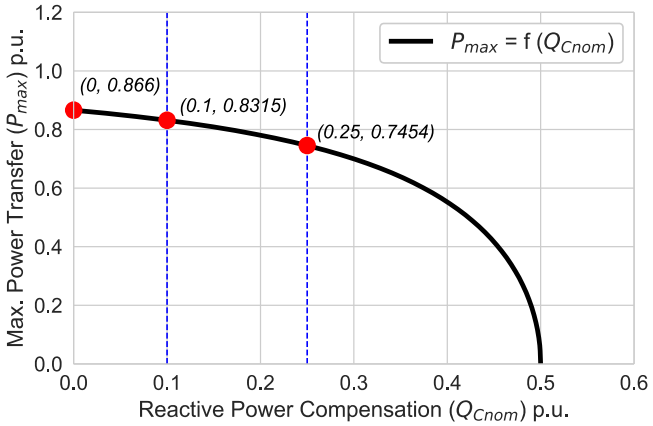

Figure 4. Maximum power transfer as a function of shunt compensation normalized by the short-circuit capacity.

For no compensation, the maximum power transfer is equal to 0.866 per unit, as expected from (16). However, as more reactive compensation is added, maximum power transfer drops. For $Q_{C_{nom}} = 0.1$ (0.25) pu, the maximum power transfer drops to 0.8315 (0.7454) pu, respectively.

To understand these effects, two aspects are important. Capacitors increase system impedance, as per (19). This reduces system strength. However, they also boost the voltage by injecting reactive power, which increases system strength. Fig. 5 shows the comparison for the *same* voltage level, i.e. given the same voltage, the bus with less compensation needed to achieve that voltage is the stronger bus. If it is, however, assumed that adding a capacitor would increase the voltage, the maximum power transfer could increase. To showcase this, two illustrative cases are considered and visualized using (22); the first one with a nominal voltage $V_i = 1\,pu$, and the second one with an assumption that the shunt capacitor boosts the voltage to $V_i = 1.1\,pu$. The results are shown in Fig. 5.

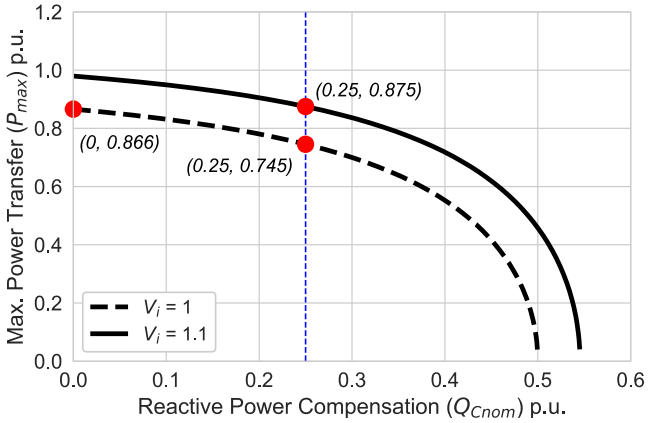

Figure 5. Maximum power transfer as a function of shunt compensation normalized by short-circuit capacity. Impact of a different operating voltage.

In this case, the addition of a capacitor was able to increase the maximum power transfer from 0.866 to 0.875 pu. However, to maintain voltage stability, the operating voltage had to be increased from $V_i = 1$ to $V_i = 1.1\ pu$. If the voltage remains the same, the maximum power transfer would decrease to 0.745 pu.

Therefore, capacitors have two opposing effects on system strength. They increase system impedance (negative effect) but also increase operating voltage (positive effect). Which effect would be dominant depends on the system parameters, and it can be evaluated using (22). Simplified methods such as ESCR ignore these intricacies and may over- (under-) estimate system strength. The derived expressions are validated in Section IV.

C. *Impact of the X/R ratio on system strength*

Finally, it is explored how the X/R ratio affects maximum power transfer and associated system strength. If $R \neq 0$, (6) is no longer valid, and (4) and (5) should be used. However, the boundary condition defined by (11) is still applicable, as it is derived for any R. Therefore, (11) is integrated into (4) and (5). For simplicity, we define M and N, keeping in mind the θ_{max} derived in (11), as well as the mentioned trigonometric identity.

$$M = V_i^2 - V_i V_s cos\theta_{max} = V_i^2 - \frac{V_s^2}{2} \tag{24}$$

$$N = V_i V_s sin\theta_{max} = V_i V_s \sqrt{1 - \left(\frac{1}{2}\frac{V_s}{V_i}\right)^2} \tag{25}$$

Boundary active power transfer and its corresponding necessary reactive power can now be expressed as follows:

$$P_{\max(R\neq 0)} = \alpha M + \beta N \tag{26}$$

$$P_{\max(R\neq 0)} = \frac{R}{Z^2}\left(V_i^2 - \frac{V_s^2}{2}\right) + \frac{X}{Z^2} V_i V_s \sqrt{1 - \left(\frac{1}{2}\frac{V_s}{V_i}\right)^2} \tag{27}$$

$$Q_{\mathrm{P=P_{max}}(R\neq 0)} = \beta M - \alpha N \tag{28}$$

$$Q_{\mathrm{P=P_{max}}(R\neq 0)} = \frac{X}{Z^2}\left(V_i^2 - \frac{V_s^2}{2}\right) - \frac{R}{Z^2} V_i V_s \sqrt{1 - \left(\frac{1}{2}\frac{V_s}{V_i}\right)^2} \tag{29}$$

From (26), the boundary transfer is increased by the value αM, implying that system strength is increased with $R > 0$. However, careful observation reveals that the expression βN is not the same as (13) due to $X \neq |\underline{Z}|$. The impact of resistance, therefore, becomes more intricate. To shed light on this, Fig. 6 plots the dependence $P_{\max(R\neq 0)} = f(X, X/R)$, with the X-axes depicting the system reactance X and the X/R ratio. For $X \approx 1$ ($X/R \to \infty$), the maximum power transfer is equal to 0.866, in line with (13) and Section II. However, the function $P_{\max(R\neq 0)} = f(X)$ reaches a maximum ($P_{\max(R\neq 0)} = S_{sc} = 1\ pu$) for $X = 0.866$, where $X/R = 1.7321$. Hence, decreasing the X/R ratio from a very high value towards 1.7321 increases the maximum active power transfer from 0.866 to 1 per unit (from the red dot on the right towards the left one in Fig. 6).

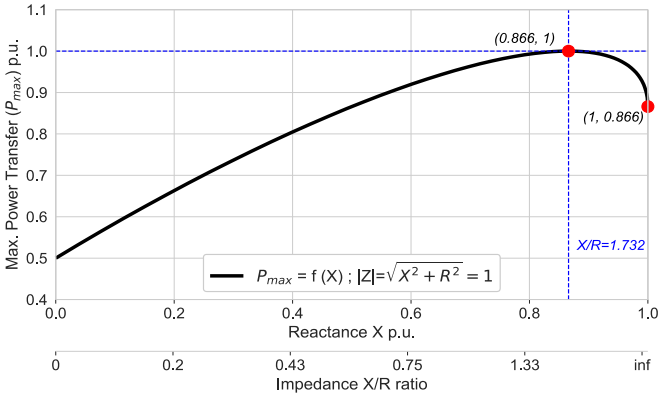

Figure 6. Maximum power transfer as a function of the X/R ratio.

However, the relationship is concave, with a peak. In other words, $P_{\max(R\neq 0)}$ drops with a further decrease of X/R. For a fully resistive system, maximum power transfer drops to only 0.5 pu. The derived analytical expressions for $P_{\max(R\neq 0)}$ and $Q_{\mathrm{P=P_{max}}(R\neq 0)}$ are validated with simulations in Section IV.

The question arises whether the ratio $X/R = 1.7321$ is a constant parameter that allows for peak maximum power transfer in every case. The answer is no, as the peak ratio also depends on the operating voltage V_i. This is demonstrated in Fig. 7, by plotting the $P_{\max(R\neq 0)} = f(X, X/R)$ dependence for typical operating voltage range $V_i = [0.9 - 1.1]\ pu$.

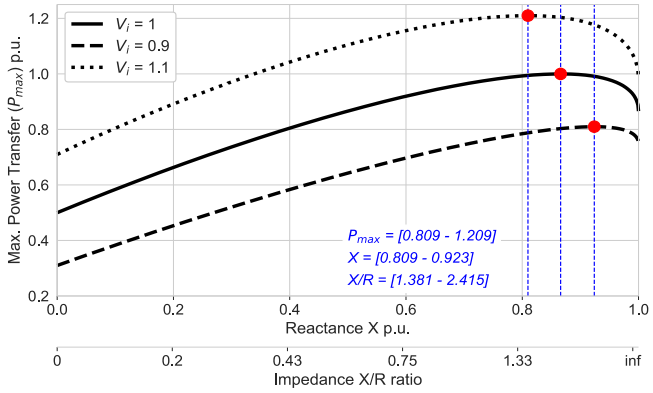

Figure 7. Maximum power transfer as a function of the X/R ratio and voltage.

From Fig. 7, the maximum active power transfer occurs at $X/R = 1.381(2.415)$ for $V_i = 0.9\ (1.1)$. Therefore, the optimal X/R ratio for peak maximum active power transfer takes a value in the range $[1.381 - 2.415]$, depending on the steady-state operating voltage. The common assumption that a relatively larger resistance increases maximum power transfer capacity is hence only valid up to a point, after which the opposite occurs.

IV. Excess system strength method

In Sections II and III it is shown that SCR is an incomplete method that may significantly overestimate system strength. In this section, a new method for system strength evaluation is introduced, based on the analytical description of the voltage collapse boundary obtained in Sections II and III. The *Excess System Strength (ESS)* method is hereby introduced. It is defined in (30), based on the balance of system strength supply and demand, normalized by the bus short-circuit capacity S_{SC}.

$$ESS = \frac{SS_{supply} - SS_{demand}}{S_{SC}} \tag{30}$$

For the bus to maintain voltage stability, there needs to be an excess of system strength available:

$$ESS > 0 \;\rightarrow\; SS_{supply} > SS_{demand} \tag{31}$$

The supply of system strength is defined as the maximum possible power transfer at the bus, considering impedance, capacitors and X/R ratio. Therefore, equations (13), (22) or (27) are to be used for P_{max}. Equation (33) exemplifies this for (13).

$$SS_{supply} = P_{max} \quad ; \quad SS_{demand} = P_{IBR} - P_L \tag{32}$$

$$ESS = \frac{1}{S_{sc}}\left[\frac{1}{X}V_i V_s \sqrt{1 - \left(\frac{1}{2}\frac{V_s}{V_i}\right)^2} - P_{IBR} + P_L\right] \tag{33}$$

The ESS method is hereby tested against two common system strength evaluation methods, SCR and ESCR. A simple model shown in Fig. 8 is simulated in DIgSILENT PowerFactory 2022. The IBR is modelled as a PQ source using the IEC Wind Generator Type 4B model [20].

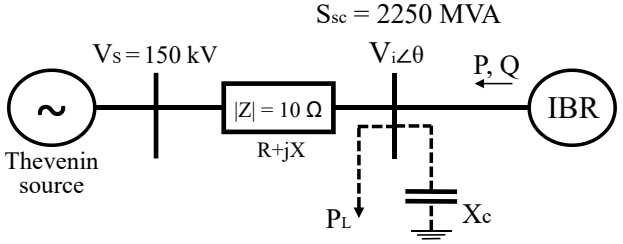

Figure 8. Simple test system for system strength evaluation.

Table 1 shows 20 scenarios selected to reflect various operating conditions. In cases A1-A3, methods are compared on a system with $P_L = 0, X_c = 0,$ and $R \approx 0$. For case A1, $1000\,MW$ is transferred. Both SCR and ESS indicate voltage stability, which is validated by simulations. Note that the ESS value indicates that an extra $948.5\,MW$ can be transferred ($0.4216 * S_{SC}$), which is also the boundary voltage stability condition in simulations. When the power increases to the boundary ($1948.5\,MW$), SCR remains larger than 1, incorrectly indicating that more power can be transferred. Meanwhile, ESS is near 0, correctly indicating the boundary condition. If the power increases further by only $1.5\,MW$ (A3), the voltage collapses. This is accurately predicted by a negative ESS, while SCR is still larger than 1, overestimating system strength. SCR implies that $2250\,MW$ can be transferred, equal to S_{SC}. However, as per derivations in Section II, this is unfeasible.

Simulations B1-B4 explore the impacts of the operating voltage. For case B1, which is the same as A1 with $1000\,MW$, but now with $V_i = 0.95\,pu$, SCR has the same value as in A1. Thus, SCR is insensitive to the change in voltage as it is typically calculated with nominal values. In contrast, ESS is 0.3633, indicating an extra $\sim 817.5\,MW$ of capacity available ($0.3633 * S_{SC}$). By increasing power to the boundary condition, it is found that precisely $1817.5\,MW$ is the maximum power transfer (MPT) at $V_i = 0.95\,pu$, as predicted by ESS. Meanwhile, SCR is still larger than 1 (1.238), wrongly indicating that the system is far from a voltage collapse. If the power experiences further increase (B3), a voltage collapse occurs, as predicted by negative ESS. SCR is, however, still positive, overestimating system strength. In case B4, the operating voltage is increased to $\sim 1.15\,pu$. Here, simulations show that the MPT is $2330\,MW$, i.e. more than what SCR suggests. Therefore, SCR can also underestimate system strength by not taking into account the operating voltage. ESS is conversely able to pinpoint the MPT, even with variable V_i.

In cases C1 (C2), a 400 (600) MW load is introduced. Based on the boundary voltage stability results, the MPT is 2348.5 (2548.5) MW, respectively. This is equal to case A2 with the addition of load, as predicted by (17). Therefore, while SCR labels these cases as unstable, ESS correctly characterizes them as boundary cases. In other words, ESS is, unlike SCR, able to consider the positive impact of load on system strength.

Simulations D1-D3 show how capacitance impacts system strength. A shunt capacitor with $Q_{C_{nom}} = 250\,MVAr$ is added, and system strength is evaluated for three different voltages. In case D1, the MPT for $V_i = 1\,pu$ is found in simulations. In this case, SCR overestimates system strength, while ESCR, designed to consider capacitors, performs better. However, it still inaccurately indicates that there is some power transfer margin left. ESS locates the boundary condition accurately, as per (22), perfectly matching simulations. In cases D2 and D3, simulations are repeated for $V_i = 0.9\,(1.1)\,pu$, respectively. ESCR is unable to accurately find the boundary condition, overestimating (underestimating) system strength in D2 (D3). On the other hand, ESS is again able to precisely match the boundary condition, and thus perform much better.

Finally, cases E1-E8 show the impact of resistance on system strength. Cases E1-E3 show the operation for the ratio $X/R = 10$. For case E1, one already sees a problem for SCR, as it is equal to case A1, where $R \approx 0$. Meanwhile, ESS predicts that an extra $\sim 1050.75\,MW$ ($0.4670 * S_{SC}$) of transfer is possible before a voltage collapse (note the difference with case A1). Indeed, simulations confirm that $2050.8\,MW$ is the boundary condition for voltage stability, as seen from case E2. If power is increased further (E3), a voltage collapse occurs. SCR fails in evaluating this, while ESS predicts the voltage collapse point accurately. Simulations E4-E6 evaluate the impact of the X/R ratio on power transfer. When the ratio decreases from 10 to 5 (E2 to E4), the MPT is increased. The same occurs when the X/R ratio is decreased to 2 (E5). However, when the X/R ratio further decreases to 1 (E6), the MPT in simulations *decreases*, as predicted in Section II-c (Fig. 7). Therefore, the expressions for ESS correctly evaluate the impact of the X/R ratio on system strength, as per E1-E6. Meanwhile, SCR falls short in determining the MPT as it does not consider the X/R ratio. This is emphasized further in cases E7 (E8), where $V_i = 0.9\,(1.1)\,pu$, with a $500\,MW$ load in the latter case. SCR significantly over-(under-) estimates system strength in these two scenarios.

TABLE I. SIMULATION RESULTS BASED ON FIG. 8 SYSTEM, COMPARING DIFFERENT SYSTEM STRENGTH METRICS OVER VARIOUS OPERATING SCENARIOS.

Operating scenario	P_{IBR} [MW]	Q_{IBR} [MVAr]	V_i [kV]	θ [deg]	P_L [MW]	$Q_{C_{nom}}$ [MVAr]	X/R	SCR	$ESCR$	ESS	Voltage collapse
A1	1000.0	234.5	150.0	26.39	0	0	inf.	2.250	-	0.4216	No
A2	1948.5	1124.9	150.0	59.99	0	0	inf.	*1.154*	-	≈ 0.001	Boundary
A3	1950.0	-	150.0	-	0	0	inf.	**1.153**	-	**-0.0006**	**Yes**
B1	1000.0	142.5	142.5	27.89	0	0	inf.	2.250	-	0.3633	No
B2	1817.5	905.6	142.5	58.23	0	0	inf.	*1.238*	-	≈ 0.001	Boundary
B3	1850.0	-	142.5	-	0	0	inf.	**1.216**	-	**-0.0144**	**Yes**
B4	2330.0	1850.3	172.6	64.15	0	0	inf.	0.965	-	≈ 0.001	Boundary
C1	2348.5	1124.9	150.0	59.86	400	0	inf.	*0.958*	-	≈ 0.001	Boundary
C2	2548.5	1124.9	150.1	59.87	600	0	inf.	*0.882*	-	≈ 0.001	Boundary
D1	1860.3	734.3	150.1	55.71	0	250	inf.	*1.209*	*1.075*	≈ 0.001	Boundary
D2	1722.5	539.37	142.5	53.68	0	250	inf.	*1.306*	*1.161*	≈ 0.001	Boundary
D3	2126.9	1154.3	165.0	59.21	0	250	Inf.	*1.057*	*0.940*	≈ 0.001	Boundary
E1	1000.0	126.9	150.0	25.89	0	0	10	2.250	-	0.4670	No
E2	2050.8	925.5	150.0	59.93	0	0	10	*1.097*	-	≈ 0.001	Boundary
E3	2055	-	150.0	-	0	0	10	**1.094**	-	**-0.0018**	**Yes**
E4	2131.3	721.0	150.0	59.99	0	0	5	*1.056*	-	≈ 0.001	Boundary
E5	2245.9	134.8	150.0	59.95	0	0	2	1.002	-	≈ 0.001	Boundary
E6	2173.3	-582.3	150.0	59.91	0	0	1	*1.035*	-	≈ 0.001	Boundary
E7	1683.8	-697.4	135.1	56.19	0	0	1	*1.336*	-	≈ 0.001	Boundary
E8	3188.4	-429.2	165.0	62.91	500	0	1	*0.706*	-	≈ 0.001	Boundary

Conversely, ESS once again precisely matches the boundary voltage collapse point found in simulations.

These simulations verify the analytical results derived in Sections II and III and show that ESS is a much more accurate measure of the steady state system strength. SCR (ESCR) can significantly over- or under-estimate system strength, as they are not able to accurately take into account impacts of voltage, loads, capacitors and X/R ratio. Meanwhile, ESS is shown to be very accurate, in line with the detailed analytical expressions for maximum power transfer. Therefore, it can be concluded that ESS is a far more suitable measure of system strength.

V. CONCLUSION

The importance of accurate system strength evaluation in progressively weaker grids is only increasing. In this paper, a new system strength method is proposed, based on a rigorous analytical derivation of IBR maximum active power transfer. Unlike existing SCR-based methods, the proposed method also considers voltage, loads, capacitors, and X/R ratio accurately. Simulation results confirm superior performance at identifying the power transfer margin and the voltage collapse point.

The method can be used as a replacement or a complement to SCR for a more accurate evaluation of system strength and voltage stability limits in a variety of operating scenarios. This ultimately allows for more robust renewables integration planning, as well as screening for weak buses with potential voltage instability risks. For future work, ESS will be expanded to consider the impact of multiple IBRs on system strength. Additionally, incorporating the impact of contingencies and IBRs' small-signal stability limits into ESS shall be explored.

REFERENCES

[1] IEEE PES-TR68, "Impact of Inverter-Based Generation on Bulk Power System Dynamics and Short-Circuit Performance", July 2018.

[2] A. Boričić, J. L. R. Torres, M. Popov. "Fundamental Study on the Influence of Dynamic Load and Distributed Energy Resources on Power System Short-Term Voltage Stability", *International Journal of Electrical Power & Energy Systems*, 2021.

[3] IEEE PES-TR77, "Stability definitions and characterization of dynamic behavior in systems with high penetration of power electronic interfaced technologies", April 2020.

[4] A. Boričić, J. L. R. Torres, M. Popov. "Comprehensive Review of Short-term Voltage Stability Evaluation Methods in Modern Power Systems", *Energies* 2021.

[5] CIGRE WG B4.62 671, "Connection of wind farms to weak AC networks", *Technical Report, CIGRE*, 2016.

[6] B. Badrzadeh, Z. Emin, S. Goyal, et al. "System Strength", *CIGRE Science&Engineering Journal*, Volume No.20, February 2021.

[7] M. G. Dozein et al. "System Strength and Weak Grids: Fundamentals, Challenges, and Mitigation Strategies," *AUPEC,* 2018.

[8] GHD Advisory, "Managing System Strength during the Transition to Renewables", ARENA project report, Australia, April 2020.

[9] A. Boričić, J. L. R. Torres, M. Popov. "System Strength: Classification, Evaluation Methods, and Emerging Challenges in IBR-dominated Grids", *IEEE Innovative Smart Grid Technologies (ISGT) Asia*, 2022.

[10] AEMO, "System Strength Requirements Methodology", Dec. 2022.

[11] A. Boričić, J. L. R. Torres, M. Popov, "Quantifying the Severity of Short-term Instability Voltage Deviations", *International Conference on Smart Energy Systems and Technologies (SEST)*, Sept. 2022.

[12] A. Haddadi, E. Farantatos, I. Kocar, and U. Karaagac, "Impact of Inverter Based Resources on System Protection", *Energies*, Feb. 2021.

[13] A. Boričić, J. Wang, Y. Li, et al. "Impact on Power System Protection by a Large Penetration of Renewable Energy Sources", *18th Wind Integration Workshop*, Oct. 2019.

[14] NERC "Integrating Inverter-Based Resources into Low Short Circuit Strength Systems - Reliability Guideline", Dec. 2017.

[15] T. Lund, H. Wu, H. Soltani, et al. "Operating Wind Power Plants under Weak Grid Conditions Considering Voltage Stability Constraints", *IEEE Transactions on Power Electronics*, Sept. 2022.

[16] F. Zhang, H. Xin, D. Wu, et al. "Assessing Strength of Multi-Infeed LCC-HVDC Systems Using Generalized Short-Circuit Ratio", *IEEE Transactions on Power Systems*, 2019.

[17] A. Ekic, B. Strombeck, Di. Wu and G. Ji, "Assessment of Grid Strength Considering Interactions between Inverter-based Resources and Shunt Capacitors", *IEEE Power & Energy Society General Meeting*, 2020.

[18] D. Wu, G. Li, M. Javadi, et al. "Assessing Impact of Renewable Energy Integration on System Strength Using Site-Dependent Short Circuit Ratio", *IEEE Transactions on Sustainable Energy*, 2018.

[19] S. Achilles, "Weak grid connection of IBR, why are we still talking about this?" G-PST/ESIG Webinar, Nov. 2021.

[20] IEC 61400-27-1 "Electrical Simulation Models for Wind Power Generation", 2020.